New Conjugated Ladder Polymer Containing Carbazole Moieties

ARTICLE *in* ADVANCED FUNCTIONAL MATERIALS · AUGUST 2003

Impact Factor: 11.81 · DOI: 10.1002/adfm.200304344

ADVANCED FUNCTIONAL MATERIALS

New Conjugated Ladder Polymer Containing Carbazole Moieties**

By *Satish A. Patil*, *Ullrich Scherf**, and *Andrey Kadashchuk**

A new ladder polymer incorporating a polar carbazole group within the main chain, ladder-type poly(*para*-phenylene carbazole), LPPPC, was synthesized and characterized by luminescence techniques. Its properties are compared to that of the well-known methyl-substituted ladder-type poly(*para*-phenylene), MeLPPP. The results obtained evidence a very low energetic disorder in this new polymer, presumably due to its near-perfect intrachain structure and low content of defects. It was found that although the density of states (DOS) distribution for neutral excitations is narrower than in MeLPPP, the manifold of charge-transporting localized states is substantially more energetically disordered due to important dipolar disorder contributions.

1. Introduction

Aromatic ladder polymers possess a unique set of characteristic properties due to their planar structure. The molecules are more resistant to deformation and thermal softening. However, they have seemed to have no practical utility because of the difficulties in processing them. In the past 10 years, novel ladder polymers with solubilizing side chains have been synthesized. Such ladder polymers have been proven to be easier to process and have interesting optical and electronic properties. In 1991 the first poly(*para*-phenylene)-type conjugated ladder polymer (LPPP) was synthesized and it was found that this polymer can be used as an active layer in organic light-emitting diodes (OLEDs) and polymer lasers.[1–7]

However, LPPP is an non-polar polymer without a permanent dipole. We have synthesized successfully a new ladder-type polymer poly(*para*-phenylene carbazole) (LPPPC) including the polar carbazole group within the main chain. The permanent dipole moment within the repeat unit is expected to be useful for many optoelectronic applications (e.g., as two-photon absorber). In this paper, we report the synthesis of LPPPC and some preliminary studies of the electronic and optical properties. This class of new ladder polymers is particularly promising for the future development of light-emitting diodes, polymer lasers, and optical limiters.

[*] Prof. U. Scherf, S. A. Patil
Bergische Universität Wuppertal
Makromolekulare Chemie
Gauss-Str. 20, D-42097 Wuppertal (Germany)
E-mail: scherf@uni-wuppertal.de
Dr. A. Kadashchuk
Institute of Physics
National Academy of Sciences of Ukraine
Prospect Nauki 46, 03028 Kiev (Ukraine)
E-mail: dmitryi@g.com.ua

[**] A. K. acknowledges financial support from NATO grant PST.CLG 978952, U.S. and S. P. from the Bundesministerium für Bildung und Forschung of Germany (BMBF). We thank Dr. Vakhnin for assistance with TSL measurements and Prof. Bässler for helpful discussions during the course of this study.

2. Results

2.1. Synthesis

The novel carbazole-based ladder polymer was generated in a three-step synthetic sequence according to Scheme 1. The first step is a Pd^0 catalyzed Suzuki cross-coupling for the synthesis of the single-chain polyarylene **3**. The Pd^0-catalyzed poly-

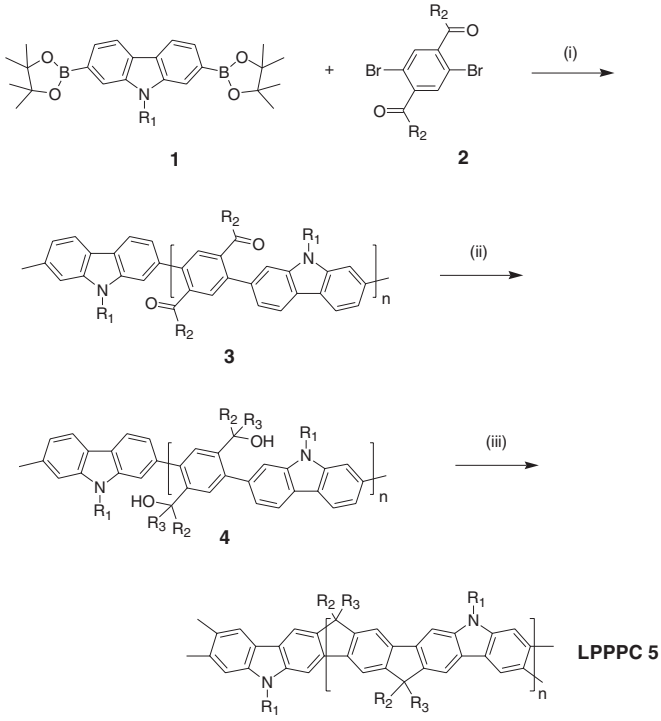

Scheme 1. Synthesis of ladder poly(*para*-phenylene carbazole) (LPPPC).

condensation reaction of *N*-octyl-2,7-bis(4,4,5,5-tetramethyl-1,3,2-dioxaborolan-2-yl)carbazole (**1**)[8] with the dibromo terephthalophenone derivative **2** provides the polyketone **3**. The ^{13}C NMR spectrum of **3** displays 14 signals of non-equivalent carbons in the aromatic/carbonyl region. In order to synthesize the desired ladder polymer the polyketone **3** was first transformed into the polyalcohol **4** by reaction with Me-Li. The final ring closure reaction of **4** to the planar ladder polymer **5** was

 DOI: 10.1002/adfm.200304344

carried out in dichloromethane with boron trifluoride etherate as the Lewis-acid catalyst. Immediately after the addition of BF_3 a strong blue fluorescent solution is obtained indicating the formation of the ladder polymer **5**. The ring closure occurs at the electronically activated 3- and 6-positions of the carbazole system. The ladder polymer **5** is completely soluble in common organic solvents (e.g., chloroform, toluene). The ^{13}C NMR spectrum of **5** displays the expected 13 signals of non-equivalent aromatic carbons (see the Experimental section). The number and weight average molecular weights of **5** (gel permeation chromatography (GPC), polystyrene (PS) calibration) were estimated to be 35 300 and 69 100, respectively, which corresponds to an average degree of polymerization of ca. 45 repeat units.

2.2. Photoluminescence Studies

The room-temperature absorption and photoluminescence (PL) spectra of LPPPC **5** in chloroform solution are shown in Figure 1. Both spectra exhibit a characteristic fine structure. The $S_0 \rightarrow S_1$ (0–0) transition is centered at 460 nm (2.64 eV),

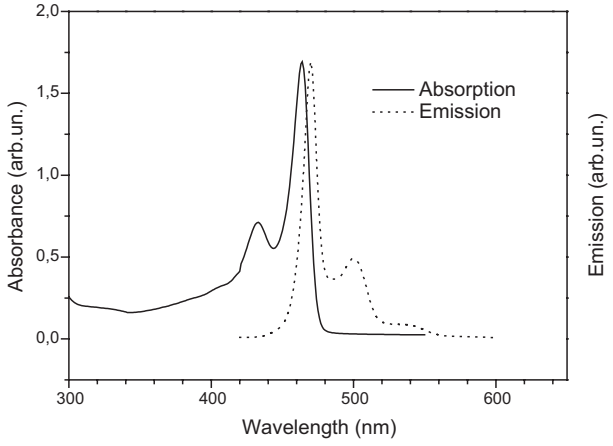

Fig. 1. Absorption and emission spectra of LPPPC ($CHCl_3$, dilute solution).

accompanied by a vibronic feature displaced by 0.19 eV to higher energy. The low-energy tail of the absorption spectrum can be fitted with a Gaussian function with a width, σ, of ca. 0.029 eV (235 cm^{-1}) that is slightly smaller than that of MeLPPP (0.033 eV, 270 cm^{-1}) and considerably smaller than the value of 650 cm^{-1} reported for PPV.[9] Thus, similarly to MeLPPP, LPPPC **5** is a polymer with greatly reduced disorder. The PL spectrum of LPPPC **5** is the mirror image of the absorption spectrum ($\lambda_{max} = 468$ nm). The small Stokes shift of ca. 0.057 eV (460 cm^{-1}, upon excitation under non-site-selective conditions) in LPPPC **5** (Table 1) testifies to the rigid geometry of this ladder polymer. The absorption and emission spectra of LPPPC **5** shows a pronounced 0–0 transition, the absorption and emission maxima are slightly red-shifted in relation to the corresponding nitrogen-free ladder polymer MeLPPP (see chemical structure below) due to the presence of the electron-donating >NR substituents of the carbazole moieties within the conjugated main chain.

Table 1. UV-vis and photoluminescence data of MeLPPP and LPPPC.

Polymer	M_n/M_w [a]	Absorption max. λ_{max} [c] [nm]	Emission max. λ_{max} [c] [nm]
MeLPPP	38.500/76.100 [b]	446	460
LPPPC 5	35.300/69.100 [b]	460	470

[a] GPC, PS calibration. [b] After removal of oligomers by extraction with acetone. [c] Dilute solution, $CHCl_3$.

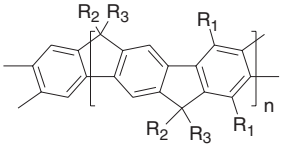

MeLPPP

$R_1 = n\text{-}C_6H_{13}$; $R_2 = 1,4\text{-}C_6H_4\text{-}n\text{-}C_{10}H_{21}$; and $R_3 = CH_3$

It is worth noting that the prompt fluorescence (PF) spectrum of a frozen, diluted solution of LPPPC **5** measured at 4.2 K is substantially better resolved than that at room temperature (Fig. 2), and consists of a main $S_1 \rightarrow S_0$ band at 484 nm (2.56 eV) followed by at least four well-resolved vibronic features displaced by about 80, 160, and 350 meV, accordingly. As expected, the low-temperature PF spectrum of a LPPPC film is less resolved than that in solution (for instance, the emission band at 500 nm is no longer resolved in the PF spectrum of the film). Apart from the somewhat better resolved structure and the apparent red shift upon lowering the temperature, the PF spectrum of LPPPC at 4.2 K is essentially similar to that measured at room temperature (see Fig. 1).

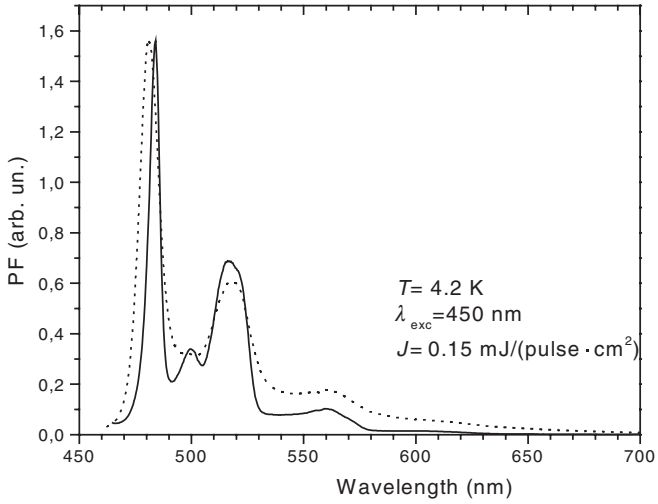

Fig. 2. Prompt fluorescence (PF) measured at 4.2 K in both frozen, dilute solution (solid line; solvent: toluene) and in a film of LPPPC (dotted line).

Low-temperature delayed emission spectra of LPPPC detected by introducing a time delay between the exciting laser pulse and the detection window of the registration system are presented in Figure 3. The spectra in Figure 3 were measured with different time delays (indicated in the Figure) and a registration gate width of 10 ms. In contrast to the PF spectra, the delayed emission from both LPPPC solution (Fig. 3a) and film (Fig. 3b) exhibits two different sets of bands with different de-

ADVANCED FUNCTIONAL MATERIALS

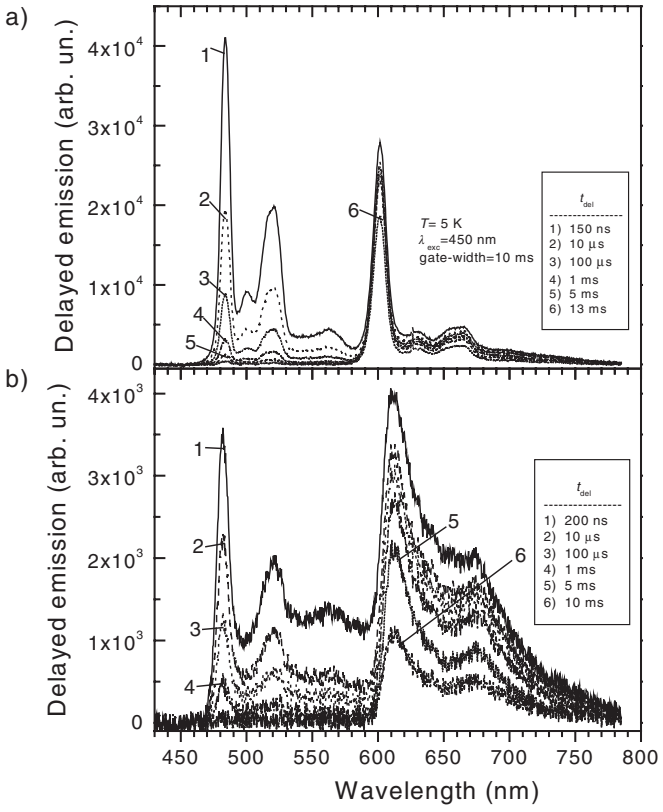

Fig. 3. Delayed fluorescence (DF) and phosphorescence (Ph) measured at 4.2 K in frozen, dilute toluene solution (a) and in a LPPPC film (b). $\lambda_{exc} = 450$ nm, laser power ≈ 0.15 mJ pulse^{-1} cm^{-2}), gate width = 10 ms, time delay is indicated in the Figure.

cay times and different spectral positions. The shorter-wavelength part of the delayed emission of the dilute solution consists of four pronounced bands ranging from 470 to 570 nm (Fig. 3a) and is virtually identical to the PF spectrum of LPPPC (Fig. 2). Thus this can be assigned to the delayed fluorescence (DF) from the S_1 state of LPPPC chain. The second slower decaying set of bands is shifted by 0.5 eV with respect to the first peak of the DF, but has the same vibrational structure (Fig. 3a) as the fluorescence spectrum. It should be noted that this second series of bands can be seen only in the delayed emission and shows all generic signatures of phosphorescence, principally similar to that previously found in MeLPPP.[10,11] Therefore we assign this spectral part to phosphorescence from the T_1 state of LPPPC, with a singlet–triplet (S_1–T_1) splitting of about $\Delta E_{ST} = 0.5$ eV, which probably is the smallest value observed so far in conjugated polymers. The above S_1–T_1 gap value for LPPPC may be due to a large effective conjugation length in this polymer, as the gap decreases with increasing conjugation of the polymer backbone for PPP-type polymers.[12]

The DF in diluted LPPPC solutions decays considerably faster than phosphorescence and it is hardly detectable after a time delay of some tens of milliseconds, while the phosphorescence decreases by about a factor of two more slowly and dominates in the millisecond domain (Fig. 3a). The detailed study of the origin of DF as well as the decay kinetics of DF and phosphorescence in LPPPC will be presented elsewhere.

Delayed emission of LPPPC film is also due to DF and phosphorescence (Fig. 3b) however some differences should be mentioned. First, both DF and phosphorescence spectra in the solid film are less resolved than in dilute solution. Second, phosphorescence bands are notably broader and shifted to lower energy, thus leading to a slightly larger S_1–T_1 gap of $\Delta E_{ST} = 0.55$ eV.

2.3. Thermally Stimulated Luminescence in LPPPC

Thermally stimulated luminescence (TSL) has proved to be a suitable technique for studying the trapping effects in disordered organic materials.[13,14] TSL can provide important information on both the intrinsic density of states (DOS) and also extrinsic deep trap distributions in conjugated polymers.[15–18] Recently, TSL was observed in MeLPPP.[15] Radiative recombination of sufficiently long range photogenerated off-chain geminate pairs of charge carriers has been identified as the origin of TSL in these materials. Figure 4 shows a typical TSL curve of a LPPPC film (curve 1) after excitation at 4.2 K for a few minutes; the TSL of a MeLPPP film monitored under the same

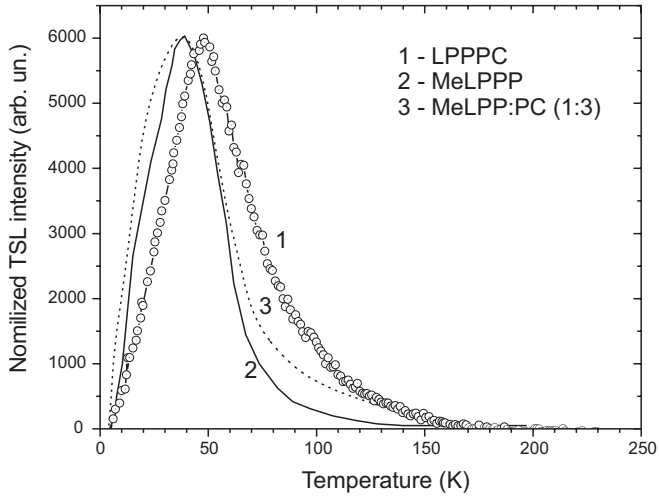

Fig. 4. Typical TSL curve of LPPPC (curve 1) and MeLPPP films (curve 2) monitored under the same conditions. Curve 3 shows TSL for a blend MeLPPP/PC (1:3).

conditions is given for comparison (Fig. 4, curve 2). TSL of LPPPC represents a broad single peak with the maximum at $T_m \approx 50$ K and the TSL occurs only at relatively low temperatures, as expected for a weakly disordered material devoid of deep traps. However, as one can see from Figure 4, the TSL glow curve of LPPPC film is broader and notably extended to higher temperatures in comparison to that of MeLPPP. This suggests a larger concentration of energetically "deeper" tail states and concomitantly somewhat larger energetic disorder of the charge-transporting manifold in this material.

Fractional TSL measurements revealed a quasi-continuous localized state distribution in LPPPC film similar to that we found before in MeLPPP (see Kadashchuk et al. for details).[15] As with the previously studied MeLPPP, the mean TSL activa-

tion energy, $\langle E_a \rangle$, in LPPPC films also increases linearly with increasing temperature according to the empirical equation which, within the experiment errors, is the same as for MeLPPP:[15]

$$\langle E_a \rangle(T) = 0.0018T - 0.016 \quad (1)$$

It should be noted that our TSL studies did not reveal any notable additional deep traps in LPPPC films. It seems that the broader TSL peak is an inherent property of LPPPC, thus reflecting somewhat enhanced intrinsic energetic disorder in this polymer rather than being affected by the presence of extrinsic traps. The observed characteristic features of TSL in LPPPC can be explained in terms of the hopping model for thermally assisted relaxation developed recently by Arkhipov et al.[16] This model describes most of the basic features of the TSL in disordered organic materials and permits the calculation of the DOS distribution from the TSL data (for details see Arkhipov et al.).[16] According to the model, TSL arises due to thermal release of charge carriers from tail states of the DOS distribution. A specific feature of disordered solids is that *intrinsic hopping states* localized within the tail of the DOS, can act as traps. As a result, the deepest portion of an energetically disordered manifold of localized states could be responsible for shallow charge trapping at very low temperatures. An effective width of the DOS of $\sigma = 0.055$ eV was approximated from the experimental TSL data on MeLPPP.[15] This value agrees reasonably well with the results of charge-transport measurements yielding $\sigma = 0.05$ eV.[19,20]

It is worth noting that the model implies[16] that the high-temperature tail of a TSL curve becomes a straight line when plotted on a $\log I$ versus T^2 scale (or $\log I$ vs. E^2 after converting the temperature scale to a trap energy scale using the empirical calibration (Eq. 1)) with a slope that is a measure of the DOS width. The results of Gaussian analysis of the high-temperature wing of the TSL peak of MeLPPP and LPPPC are presented in Figure 5 and are consistent with the above model. The high-temperature tails of TSL glow curves can be reasonably well approximated by straight lines (Fig. 5). The widths of the distributions estimated from the slopes are 0.052 and 0.9 eV for MeLPPP and LPPPC films, respectively. It worth noting that, depending on sample, two apparent straight lines could be revealed for LPPPC films (this situation is shown in Fig. 5) the slopes of which yield the widths of 0.07 and 0.09 eV at shallower and deeper energies, respectively (the linear part at smaller energies is less pronounced and is sample dependent). This observation might imply a superposition of two distributions of localized states at the tail of the cumulative DOS of LPPPC film and it merits further investigation. Here, it should be mentioned that a double-peak DOS distribution was also observed before for many photoconducting polymers.[13,16] This might have originated at least partially from medium- and long-range potential fluctuations, which are expected to be important and often taken into account for characterizing charge transport in dipolar media.[21] Since it is obvious that the lower portion of the DOS controls temperature-activated hopping, the charge transport should be controlled by the deeper distribution with the width of 0.09 eV. It should be mentioned that in the above analysis it was assumed that the effective transport energy level coincides with the center of the DOS distribution. The validity of such approximation for ladder-type polymers has been presented by Kadashchuk et al.[15]

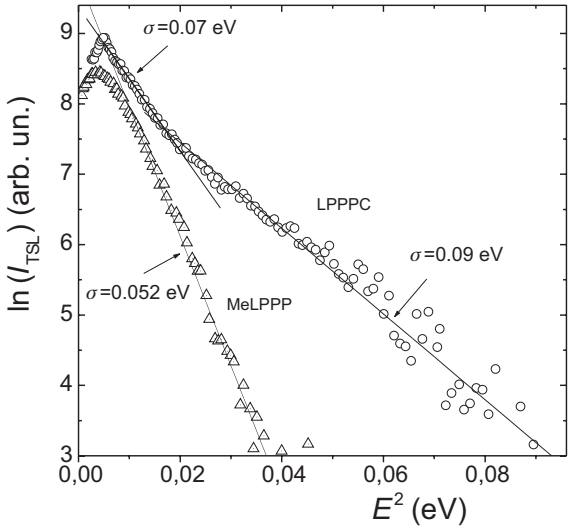

Fig. 5. Gaussian analysis of the high-energy wing of the TSL peaks of MeLPPP (triangles) and LPPPC (open circles) films.

Analyzing the TSL emission spectrum of a LPPPC film we found that both phosphorescence and DF contribute to the TSL emission and that the TSL curve shape is almost the same when monitored either via phosphorescence or DF. The major difference, however, is that the phosphorescence contribution in the TSL spectra is greater by a factor of 10 then the DF contribution, thus phosphorescence dominates in TSL emission of LPPPC films. A possible reason for such an effect has been suggested[18] as being due to the energy splitting of the singlet and triplet states of geminate charge-carrier pairs in conjugated polymers.

Finally, curve 3 in Figure 4 shows the TSL glow curve of MeLPPP doped into a polar matrix, bisphenol *A*-polycarbonate (PC, dipole moment of PC is 2.3 D). As one can see from the comparison of curves 2 and 3, the broadness of the TSL glow curve and, concomitantly, the energetic disorder, tends to increase with increasing polarity of the polymer film.

3. Discussion

LPPPC **5** is a novel ladder polymer containing a polar carbazole group within the main chain. LPPPC **5** is expected to be important for many optoelectronic applications due to the presence of a permanent dipole moment within the repeat unit, which should lead to an increase in the two-photon absorption cross-section. The luminescence characterization of this polymer revealed no evidence for defects or impurities. Absorption and PL spectra of LPPPC **5** (as an amorphous conjugated polymer) display remarkably narrow linewidths for the allowed singlet exciton transitions, which is, in principle, similar to that observed in the spectra of MeLPPP.[22] It is generally believed

ADVANCED FUNCTIONAL MATERIALS

that inhomogeneous broadening of spectral bands in conjugated polymers arises mainly from a random length variation of the conjugated segments, which are separated from each other by topological faults (which might be either of conformational or chemical origin) within the polymer chain.[23] Therefore, LPPPC is a very attractive material as far as its optical properties are concerned, since distribution of effective conjugation lengths in this polymer is very narrow. The latter is evidenced by i) a small inhomogeneity of the absorption spectra featuring a variance of $\sigma \approx 235$ cm^{-1}, even smaller than that in MeLPPP (ca. 270 cm^{-1}), ii) a small Stokes shift of 460 cm^{-1} ($\approx 2\sigma$) that is comparable to the value of 500 cm^{-1} reported for MeLPPP,[20] and iii) a very well-resolved PL spectrum featuring vibronic fine structure especially at low temperatures. The well-pronounced 0–0 transition with respect to its vibronic replica in the absorption spectrum of LPPPC **5** implies a reduced Huang–Rhys factor for LPPPC, when compared to MeLPPP.

The first triplet (T_1) state of a LPPPC film at 2.02 eV is somewhat red-shifted to that of the solution at 2.06 eV, while the DF spectra are virtually the same. The phosphorescence spectra in the film are considerably broader in comparison to those in dilute solutions of LPPPC **5**. These two observations can be readily explained by spectral diffusion of long-lived triplets towards "lower-energy" tail states within the DOS distribution. Such a diffusion in dilute, frozen solution is restricted to the migration of triplets along isolated polymer chains, and is, therefore, inefficient in reaching the lowest-energy sites. On the other hand, diffusivity of triplets is enhanced in the solid state due to interchain hopping. The triplets can reach a larger number of sites during their lifetime and thus can be trapped on "deeper" tail states. The faster decay of phosphorescence in the LPPPC film (compare Figs. 3a,b) supports such a notion since it illustrates triplet quenching at quenching centers (like oxygen) due to interchain triplet diffusion, which shortens the triplet lifetime.

The results of TSL measurements in LPPPC films initially seem to be in contradiction with the PF and DF data for this polymer. Indeed, TSL results (Figs. 4,5) suggest notably broader DOS distribution for charge carriers in LPPPC when compared to a MeLPPP film, although the DOS distribution for neutral excitations shows the opposite trend. Analysis presented in Figure 5 clearly demonstrates the larger width of the charge-carrier DOS distribution in LPPPC films. This effect can be explained with the presence of the permanent dipole moment of the carbazole moiety of LPPPC (~2 D)[24] (in contrast to the almost non-polar MeLPPP). It should be noted that similar effects were observed during the blending of dipolar additives or dipolar charge-transporting molecules into molecularly doped polymers (MDP),[25–27] or by the introduction of dipoles into σ-conjugated polysilanes[28] and polymers containing side-chain carbazole units.[29]

Dipolar effects on energetic disorder for charge carriers are well known and thoroughly studied for MDPs and other organic photoconducting materials.[25] They can be described in terms of the dipolar disorder model[26] according to Borsenberger and Bässler, which predicts a linear increase of a so-called dipolar component of disorder σ_{dip} with increasing dipole moment. Dipolar disorder arises due to electrostatic interaction of a charge carrier with randomly located and randomly oriented permanent dipoles which, in principle, might be associated either with polar charge transporting sites, polar additives, or polar polymer binders in the case of MDPs. The total width of the DOS for charge carriers is determined[26] by both a *non-polar disorder contribution* (which apparently is due to a distribution of segment lengths in conjugated polymers and the variance of the van der Waals interaction energy) σ_{np} and a *dipolar component* σ_{dip}:

$$\sigma = (\sigma_{np}^2 + \sigma_{dip}^2)^{1/2} \tag{2}$$

The dipolar component σ_{dip} (in eV) can be calculated by the following expression[27]

$$\sigma_{dip} = \frac{7.04 c^{1/2} p}{a\varepsilon} \tag{3}$$

where p is the dipole moment (in Debye (D)), c the concentration of dipoles, a the intersite distance (in Å), and ε the dielectric constant. Since MeLPPP is a non-polar polymer the dipolar disorder component is negligible. Assuming for LPPPC a dipole moment equal to that of the carbazole molecule $p = 2$ D,[24] the parameters $a = 6$ Å and $\varepsilon = 3.5$ (similar to that of MeLPPP),[30] and assuming $c \approx 0.5$, one can roughly estimate by Equation 3 the dipolar disorder contribution for this polymer as $\sigma_{dip} = 0.078$ eV. On the other hand, if one assumes the non-polar disorder component for LPPPC (as for non-polar MeLPPP) as $\sigma_{np} = 0.05$ eV, Equation 2 and the value of $\sigma = 0.09$ eV, estimated from our TSL experiment for LPPPC **5** (Fig. 5), gives a dipolar disorder component for LPPPC **5** of $\sigma_{dip} = 0.075$ eV. This value agrees well with the value of 0.078 eV calculated above with Equation 3.

Finally, it should be noted that the DOS for neutral excitations is probably much less affected by the presence of a permanent dipole moment in LPPPC and the width of the exciton manifold is determined mainly by the distribution of conjugated lengths. Besides, broadening the DOS due to dipolar fields is possible only in undiluted films provided that there are random orientations in neighboring chains. However, one should not expect such on-chain motion effects in diluted solutions. The latter is supported by the observation of very narrow PL bands in frozen diluted solutions of LPPPC.

To verify the dipolar disorder hypothesis we measured TSL also in MeLPPP doped into bisphenol *A*-polycarbonate (PC), a polar polymer matrix which has a permanent dipole moment of 2.3 D.[26] PC is used very extensively[25] to study the dipolar disorder effect in MDPs. Curve 3 in Figure 4 shows TSL measured in MeLPPP doped into PC (1:3). The TSL curve is notably shifted to higher temperatures with respect to that of the pure MeLPPP film (curve 2), which can be explained by the introduction of dipolar disorder due to the polar PC matrix.

5. Experimental

Dichloro[1,1-bis(diphenylphosphino)ferrocene]palladium(II) (dichloromethane adduct), and tetrakis(triphenylphosphino)palladium(0) were purchased from Aldrich. The solvents were dried by conventional methods, freshly distilled, and stored under argon. All reactions of air- and water-sensitive materials were performed using standard Schlenk techniques. ^{1}H and ^{13}C NMR spectra were obtained on a Bruker AMX 300 spectrometer. For gel permeation chromatography analysis (GPC) PS columns (three columns, 5 μm gel, pore width 10^3, 10^5, and 10^6 Å) connected with UV-vis/refractive index (RI) detection were utilized. All GPC analyses were performed on solutions of the polymers in tetrahydrofuran. Calibration was based on polystyrene standards with narrow molecular weight distribution. The following compounds were synthesized according to the literature: *N*-octyl-2,7-bis(4,4,5,5-tetramethyl-1,3,2-dioxaborolan-2-yl) carbazole (**1**) [8], 2,5-dibromo-1,4-bis(4-decylbenzoyl)benzene (**2**) [1].

*Synthesis of Polyketone **3***: A dried 100 mL flask was filled with the monomers **1** (531 mg, 1 mmol) and **2** (724 mg, 1 mmol) dissolved in 20 mL of toluene. Then, $Pd(PPh_3)_4$ (35 mg), Na_2CO_3 (1 g in 5 mL of distilled water), and *n*-butanol (5 mL) were added. The mixture was refluxed under argon for 3 days. The resulting white suspension was poured into cold methanol, and the precipitate collected by filtration. After being dried under high vacuum for 24 h a light yellowish solid **3** was obtained. Yield: 570 mg (67 %).

*Synthesis of Polyalcohol **4***: Me-Li (200 mg, 10 mmol, as 1.6 M solution in diethyl ether) was added under argon to a solution of the polyketone **3** (400 mg, 0.476 mmol) in a mixture of toluene and tetrahydrofuran (1:1, 100 mL). The solution was stirred for 30 min at room temperature and carefully quenched with ethanol. The organic layer was washed with water and 2 N hydrochloric acid, dried, and concentrated to dryness. The polymer **4** was dried thoroughly under high vacuum for 24 h. Yield: 310 mg (75 %).

*Synthesis of Ladder Polymer **5***: A solution of polymer **4** (250 mg, 0.286 mmol) in dichloromethane (50 mL) was treated with boron trifluoride etherate (2.896 g, 20.37 mmol). The solution was stirred for 30 min at room temperature. Then, ethanol (20 mL) was added, followed by water (50 mL) to quench excess boron trifluoride. The organic layer was carefully washed with water, dried, and concentrated. Precipitation into acetone gave polymer **5** as a yellow powder. Yield: 200 mg (83 %)

^{1}H NMR (300 MHz, $C_2D_4Cl_4$ [ppm]): δ = 7.8–7.7, 7.3–7.2 (broad), 2.6, 2.0, 1.6, 1.4, 1.3, 0.9. ^{13}C NMR (75 MHz, $C_2D_4Cl_4$ [ppm]): δ = 154.0, 146.0, 143.5, 141.1, 140.4, 140.1, 137.9, 134.2, 128.0, 126.6, 123.8, 122.7, 115.2, 53.3, 35.2, 31.5, 30.7, 29.2, 28.9, 26.5, 25.0, 22.3, 13.7. M_n: 35.3000; M_w: 69.100; M_w/M_n:1.9 (GPC, PS calibration).

LPPPC films were spin cast from chloroform or toluene solution onto a quartz substrate. The films were dried at room temperature for at least 5 h.

Spectroscopic measurements of prompt fluorescence (PF) and delayed fluorescence (DF) of both frozen, dilute solutions and films were carried out at liquid-helium temperature, 4.2 K, in a helium cryostat. Excitation was effected by a dye laser pumped with an excimer laser (duration of a laser pulse was 10 ns and repetition rate 10 Hz) at 450 nm. The emission spectra were recorded using a monochromator coupled to an optical multichannel analyzer (OMA) with a time gated, intensified diode array detector, which was synchronized by the electrical trigger of the laser. The detection window was selected between 100 ns and 10 ms. A variable delay of 200 ns to 13 ms after optical excitation allowed the detection of weak delayed luminescence after the intense prompt fluorescence. To increase the signal-to-noise ratio, spectra were accumulated by averaging over 300 pulses. Absorption and emission spectra of LPPPC at room temperature were also monitored.

The TSL measurements were carried out using a home-built system operable from 4.2 to 350 K. TSL measurements after UV light excitation were performed with two different methodologies: uniform heating at a rate $\beta = 0.15\ \mathrm{K\,s^{-1}}$, and fractional heating. The latter procedure allows the determination of trap depth when different groups of traps are not well separated in energy or are continuously distributed. The fractional TSL technique [31], being an extension of the initial rise method, is based on cycling the sample with a large number of small temperature oscillations superimposed on a constant heating ramp. The main outcome of the fractional TSL is the temperature dependence of the mean activation energy, $\langle E \rangle(T)$ [31,32]. The experimental details and the data processing procedures have been described elsewhere [13,14].

Received: January 24, 2003
Final version: April 25, 2003

[1] U. Scherf, K. Müllen, *Makromol. Chem. Rapid Commun*. **1991**, *12*, 489.
[2] W. Graupner, G. Leditzy, G. Leising, U. Scherf, *Phys. Rev. B* **1996**, *54*, 7610.
[3] S. Tasch, A. Niko, G. Leising, U. Scherf, *Appl. Phys. Lett*. **1996**, *68*, 1090.
[4] C. Kallinger, M. Hilmer, A. Haugenener, M. Perner, W. Spirkl, U. Lemmer, J. Feldmann, U. Scherf, K. Müllen, A. Gombert, V. Wittwer, *Adv. Mater.* **1998**, *10*, 920.
[5] B. Schweitzer, G. Wegmann, D. Hertel, R. F. Mahrt, H. Bässler, F. Uckert, U. Scherf, K. Müllen, *Phys. Rev. B* **1999**, *59*, 4112.
[6] J. Grüner, H. F. Wittman, P. J. Hamer, R. H. Friend, J. Huber, U. Scherf, K. Müllen, A. B. Holmes, *Synth. Met*. **1994**, *67*, 181.
[7] U. Scherf, *J. Mater. Chem.* **1999**, *9*, 1853.
[8] G. Zotti, G. Schiavon, S. Zecchin, J. F. Morin, M. Leclerc, *Macromol*. **2002**, *35*, 2122.
[9] S. Heun, R. F. Mahrt, A. Greiner, U. Lemmer, H. Bässler, D. A. Halliday, D. D. C. Bradley, P. L. Burns, A. B. Holmes, *J. Phys.: Condens. Matter*. **1993**, *5*, 247.
[10] Yu. V. Romanovskii, A. Gerhard, B. Schweitzer, U. Scherf, R. I. Personov, H. Bässler, *Phys. Rev. Lett*. **2000**, *84*, 1027.
[11] Yu. V. Romanovskii, H. Bässler, *Chem. Phys. Lett*. **2000**, *326*, 51.
[12] D. Hertel, S. Setayesh, H.-G. Nothofer, U. Scherf, K. Müllen, H. Bässler, *Adv. Mater*. **2001**, *13*, 65.
[13] A. Kadashchuk, D. S. Weiss, P. M. Borsenberger, S. Nešpuårek, N. Ostapenko, V. Zaika, *Chem. Phys.* **1999**, *247*, 307.
[14] A. Kadashchuk, N. Ostapenko, V. Zaika, S. Nešpuårek, *Chem. Phys.* **1998**, *234*, 285.
[15] A. Kadashchuk, Yu. Skryshevskii, A. Vakhnin, N. Ostapenko, V. I. Arkhipov, E. V. Emelianova, H. Bässler, *Phys. Rev. B* **2001**, *63*, 115 205.
[16] V. I. Arkhipov, E. V. Emelianova, A. Kadashchuk, H. Bässler, *Chem. Phys.* **2001**, *266*, 97.
[17] A. Kadashchuk, Yu. Skryshevski, Yu. Piryatinski, A. Vakhnin, E. V. Emelianova, V. I. Arkhipov, H. Bässler, J. Shinar, *J. Appl. Phys.* **2002**, *91*, 5016.
[18] A. Kadashchuk, A. Vakhnin, Yu. Skryshevski, V. I. Arkhipov, E. V. Emelianova, H. Bässler, *Chem. Phys*. **2003**, *291*, 243.
[19] D. Hertel, U. Scherf, H. Bässler, *Adv. Mater*. **1998**, *10*, 1119.
[20] D. Hertel, H. Bässler, U. Scherf, H. H. Hörhold, *J. Chem. Phys.* **1999**, *110*, 9214.
[21] S. V. Novikov, D. H. Dunlap, V. M. Kenkre, P. E. Parris, A. V. Vannikov, *Phys. Rev. Lett.* **1998**, *81*, 4472.
[22] M. G. Harrison, S. Möller, G. Weiser, U. Urbasch, R. F. Mart, H. Bässler, U. Scherf, *Phys. Rev. B.* **1999**, *60*, 8650.
[23] M. Pope, C. E. Swenberg, *Electronic Processes in Organic Crystals and Polymers*, 2nd ed., Oxford University Press, Oxford **1999**.
[24] A. L. McClellan, *Tables of Experimental Dipole Moments*, Freeman, San Francisco, CA **1963**.
[25] P. M. Borsenberger, D. S. Weiss, *Organic Photoreceptors for Xerography*, Marcel Dekker, New York **1998**.
[26] P. M. Borsenberger, H. Bässler, *J. Chem. Phys.* **1991**, *95*, 5327.
[27] R. F. Young, *Philos. Mag. B.* **1995**, *72*, 435.
[28] S. Nešpuårek, J. Sworakowski, A. Kadashchuk, *IEEE Trans. Dielectr. Electr. Insul.* **2001**, *8*, 432.
[29] A. Kadashchuk, N. Ostapenko, N. Lukashenko, *Adv. Mater. Opt. Electron*. **1997**, *7*, 99.
[30] V. I. Arkhipov, E. V. Emelianova, H. Bässler, *Phys. Rev. Lett*. **1999**, *82*, 1321.
[31] I. A. Tale, *Phys. Status Solidi A* **1981**, *66*, 65.
[32] P. I. Butlers, I. A. Tale, J. Pospíšil, S. Nešpuårek, *Prog. Colloid Polym. Sci*. **1988**, *78*, 93.

